JASA ARTICLE

Eigenfrequency optimisation of free violin plates[a)]

Sebastian Gonzalez,[b)] Davide Salvi, Fabio Antonacci, and Augusto Sarti
Dipartimento di Elettronica Informazione e Bioingegneria, Politecnico di Milano, Milan, Italy

ABSTRACT:
We discuss how the modal response of violin plates changes as their shape varies. Starting with an accurate 3D scan of the top plate of a historic violin, we develop a parametric model that controls a smooth shaping of the interior of the plate, while guaranteeing that the boundary is the same as the original violin. This allows us to generate a family of violin tops whose shape can be smoothly controlled through various parameters that are meaningful to a violin maker: from the thickness in different areas of the top to the location, angle, and dimensions of the bass bar. We show that the interplay between the different parameters affects the eigenmodes of the plate frequencies in a nonlinear fashion. We also show that, depending on the parameters, the ratio between the fifth and the second eigenfrequencies can be set to match that used by celebrated violin makers of the Cremonese school. As the parameterisation that we define can be readily understood by violin makers, we believe that our findings can have a relevant impact on the violin making community, as they show how to steer geometric modifications of the violin to balance the eigenfrequencies of the free plates. © *2021 Acoustical Society of America*.
https://doi.org/10.1121/10.0003599
(Received 23 September 2020; revised 3 February 2021; accepted 5 February 2021; published online 2 March 2021)
[Editor: Vasileios Chatziioannou] Pages: 1400–1410

I. INTRODUCTION

In our activity as researchers of the Musical Acoustic Lab of the Politecnico di Milano, located on the premises of the prestigious Violin Museum of Cremona, Italy, we are often asked about the "secrets" of Stradivarius (Sacconi *et al.*, 1979). The craft of violin making, in fact, is often perceived as veiled with mystique. A luthier uses just a few natural materials—spruce, maple, and ebony; animal glue to hold everything together; and sandarac, propolis, and various other resins for the varnish—and with them is able to craft an instrument that, in the hands of an accomplished performer, evokes feelings of ethereal beauty that transcend the material components of the instrument itself. Our job as researchers is to try to understand how the choice of wood (Buksnowitz *et al.*, 2007), its geometry (Tai *et al.*, 2018), and its finishing (Schelleng, 1968; Setragno *et al.*, 2017) can be "persuaded" to make this possible.

In this paper, we focus on geometric optimisation, as it is ideally suited for numerical simulations. Our goal is to develop a methodology that can be used by scientists and luthiers together that optimises the shape of the violin under given constraints.

From a mathematical standpoint, the geometry of violins is extremely complex, and the number of parameters needed to capture it with sufficient precision easily grows to an unmanageable level. To avoid this, and for reasons of didactic simplicity, we focus our attention on two specific aspects of shape optimisation: the carving of the inside of a given top plate (for a given material and outer shape) and the positioning of the bass bar in an optimal fashion, i.e., so that a given objective function is maximised. Using parameters that a luthier can control, we want to find the shape of the top plate and the position of the bass bar that optimise arbitrary functions, the idea being that once an objective function of a "good violin" has been established, we will provide violin makers with the methodology to carve the violin plates to their maximum potential.

The "geometric" standpoint has been widely pursued by researchers in musical acoustics (Bretos *et al.*, 1999; Gough, 2015; Knott *et al.*, 1989; Molin *et al.*, 1988; Staforelli *et al.*, 2002), for example, addressing the influence of the shape of the f-hole on the emitted sound (Nia *et al.*, 2015); the way the modes of the plate depend on arching, thickness, and other parameters (Gough, 2015); or how a change in the material parameters of the wood can be compensated by variations in the arching of the violin (Tinnsten and Carlsson, 2002). The use of finite element method (FEM) simulations remains the preferred method of simulation, and it is increasingly used to study real instruments (Chatziioannou, 2019; Torres *et al.*, 2020). However, to the best of our knowledge, the manipulation of laser or computed tomography (CT) scans involves a fair deal of "handwork" to turn them into usable simulation meshes. This is the main reason why we have presented our method in great detail, since we hope it will help other researchers to obtain accurate meshes easily.

The optimisation of the vibrational behavior with respect to specific objective functions has been studied occasionally in the literature. Some works have appeared in the literature concerning, for example, the design (Yu *et al.*, 2010) or the

[a)]This paper is part of a special issue on Modeling of Musical Instruments.
[b)]Electronic mail: tsuresuregusa@gmail.com

 0001-4966/2021/149(3)/1400/11/$30.00

https://doi.org/10.1121/10.0003599

compensation of parameters related to the material (Tinnsten and Carlsson, 2002). For an extensive review of violin acoustics, see Woodhouse (2014).

Some attempts have been made to relate vibroacoustics properties to "good" sound, for example, the ratio of frequencies in the free plate for modes 2 and 5, $f_5/f_2 \simeq 2.35$ for plates with f-holes and no bass bar in old Cremonese violins (Curtin, 2005; Davis, 2013), but the datasets are considerably small, and it is not clear whether such relations on the free plates survive in the complete instrument (Schleske, 1996). Furthermore, the quality of an instrument is measured by how it sounds, not how it vibrates, and in this case one should consider observables taken from perceptual experiments in the optimisation function (Fritz *et al.*, 2010, 2012, 2014).

In this work, we optimise the thickness distribution of violin plates, both with and without bass bar, for three different loss functions: t ratio f_5/f_2, a function that measures how homogeneously distributed are the frequencies (as an example of a loss function that depends on several frequencies), and finally we look to minimise the impedance of the top keeping the frequency f_5 constant (Gore and Gilet, 2016).

This study of ours differs from previous ones in several aspects. First, we start from an accurate 3D laser scan of a particularly interesting historical violin, made in 1716 by Antonius Stradivarius during his "golden period." This violin is the celebrated "Messiah," which has the peculiarities of being not only in pristine condition, but also of having been nearly untouched for over 300 years. Jean-Baptiste Vuillaume modified the neck and changed the bass bar in the 1800s, but besides that, it is "as new." For a detailed account of how the Messiah came back to Cremona and its history, see Cacciatori (2016).

Second, we approach the problem from a very luthier-centric perspective, as we control our 3D shape with parameters that are not just understood by luthiers but are actually used by them in their daily practice. This guarantees that shape variations are not only realistic but also of practical value. Third, we do not study the impact of individual parameters, but conduct our optimisation in a multidimensional parameter space to address the nonlinear interplay between parameters.

This paper is structured as follows: In Sec. II, we explain how to obtain a model of the outside of the top plate from a real violin 3D scan. In Sec. II A, we describe how the inner part of the top plate is constructed, how its thickness is varied, and how the bass bar is added to the geometry. In Sec. IV, we present the main results of the study. The conclusions are in Sec. V.

II. BUILDING A WORKING MODEL FROM A 3D SCAN

The construction of the 3D model begins with a mesh acquired through an accurate 3D laser scan of the violin. An example of laser scan of a violin is shown in Fig. 1(a). The first step is to shift and rotate the scan in such a way as to align the principal axis of the violin with the y axis of the reference frame, and to lay the top plate as best as possible with the xy plane (violin plates are not generally planar, let alone parallel). Once the positioning is complete, we can cut out the neck and the fingerboard. To "weave" a model for the surface, we now take longitudinal slices (from tailpiece to neck, along the y axis), which play the role of "warp," and fit an even polynomial to the arching along the x direction ("weft"), as shown in Fig. 2. For each value of y, we fit an even 4th-degree polynomial of the form

$$p_y(x) = a(y) + b(y)x^2 + c(y)x^4. \tag{1}$$

We therefore end up with a family of polynomials whose coefficients depend on the y coordinate, to follow the ever-changing profile of the surface. In Fig. 2, we can see how the first coefficient $a(y)$ (the height of the arching) changes as a function of y. Adding odd terms to the polynomial would be required for modeling the asymmetry of the arching (which is present in other historical examples); however, we have decided against this in the particular case of

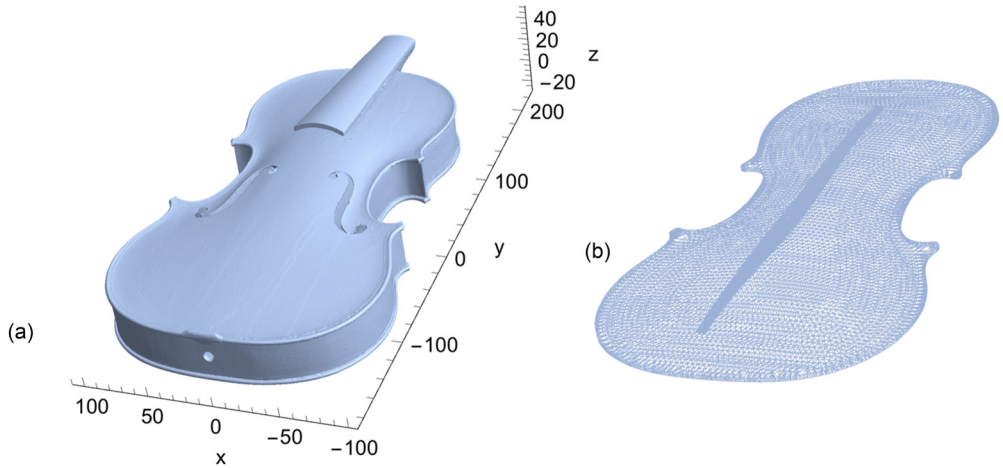

FIG. 1. (Color online) Starting point for the optimisation process. (a) 3D scan of an actual historical violin. (b) synthetic version of the violin for which the modal response is computed and then thickness is optimised via a loss function.

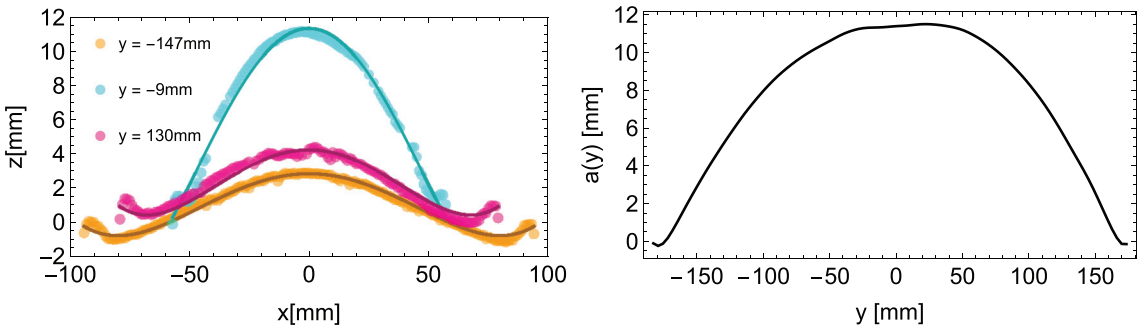

FIG. 2. (Color online) Left: with reference to Fig. 1, surface fitting for $y = -146$ mm, $y = -8$ mm, and $y = 130$ mm. The coloured points are original mesh, whereas the solid line is the fitting. Right: Coefficient $a(y)$ (height at $x = 0$) after smoothing.

the Messiah, as we do not know if the asymmetry is due to a too stressed bass bar or was original (Cacciatori, 2016). Of course, the accuracy of the fit of the parametric curve is limited by scanning errors, by possible irregularities of the surface, and by the fact that a 4th-degree polynomial can only go so far in fitting the arching. In fact, we can detect noticeable "ripples" at the borders of the synthetic mesh, which can be more or less relevant, depending on the nature and quality of the starting scan. Using higher order polynomials only increases these ripples and actually creates a worse model. The Messiah Stradivarius that we worked on was in pristine state of preservation, with a very smooth surface, which showed minimal ripples only under the fingerboard, due to inaccuracies of the laser scanning in this area, as shown in Fig. 3. To minimise the variation in the fitting parameters, we apply a smoothing operator (a low-pass filter) to the curves that describe the evolution of the coefficients as a function of y. In the case of the Stradivarius Messiah, we only need a mild smoothing of the coefficient profiles, thanks to the good condition of its surface.

The corners of the violin are removed by hand in the fitting procedure to avoid ending up with disjoint regions along the x axis. After smoothing the coefficients and removing the corners, we can proceed with building a mesh of the synthetic plate, which is suitable for numerical modeling. We do so by evaluating the fitting function $p_y(x)$ over the plate, up to a distance of 2.5 mm from the border.

To "flatten" the ripples that the polynomial base tends to generate at the borders of the plate, we multiply $p_y(x)$ with a Gaussian kernel,

$$g_y(x) = e^{-D^2/d^2},$$

where $d = x_b(y) - |x|$ is the distance of a point (x, y) to its closest edge along x, and $D > 0$ is a weight parameter that for a typical violin plate we set to 8 mm. The z coordinate of the points along the edge of the plate is then

$$z = z_p(x, y)e^{-D^2/d^2},$$

where $z_p(x, y) = p_y(x)$ is the z coordinate as modelled by the polynomial in Eq. (1).

The contour lines of the original (left) and synthetic (right) meshes of the Messiah top plate are shown in Fig. 3. One can see that the synthetic mesh is smoother and more symmetric than the mesh directly obtained from the laser scans.

With the upper surface reconstructed and smoothed, we are now able to synthesise the inner surface.

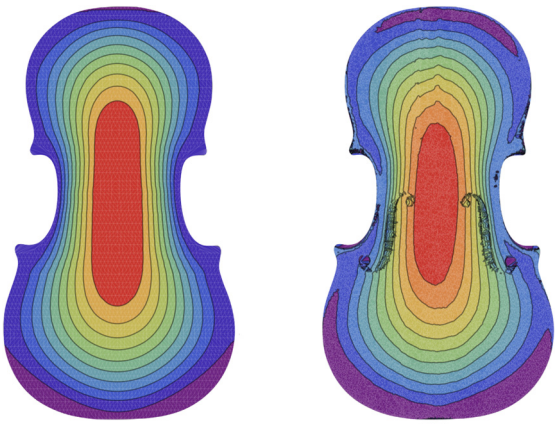

FIG. 3. (Color online) Synthetic height map (left) and actual height for the 3D scan (right) of the top plate. As one can see, the synthetic mesh is less irregular and fits the original very well. Notice how the real violin top plate does not flatten at the border: The edge of the violin is higher at the centre than at the bouts. This doming is obtained by clamping the flat top into position, which is the reason why we chose our model to be flat at the border.

A. Building the complete top plate mesh

In the process of creating the inner surface of the plate, we consider two cases. First, we approximate the thickness of the top plate in the inner part as uniform. This corresponds to a good approximation of an actual violin, as shown, for example, in Stoel and Borman (2008). Later, since we want to have full control on the plate that we are building, we will consider a more general case where we can decide to vary the thickness of the plate heterogeneously, again based on historical examples.

B. Constant thickness

The starting point of the construction process is the smoothed edge of the top, shown by the black line in Fig. 4(a). From this, we compute the internal boundary of

https://doi.org/10.1121/10.0003599

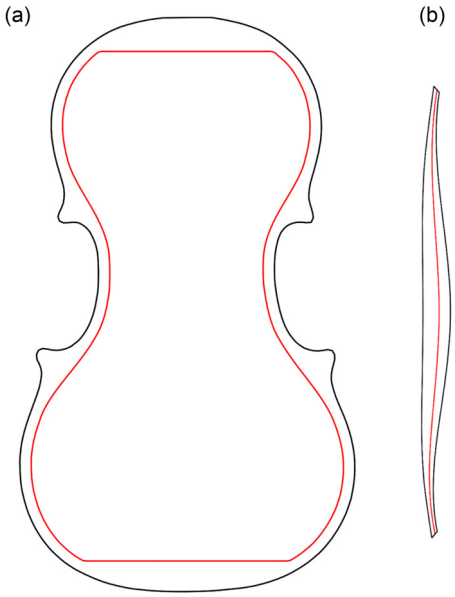

FIG. 4. (Color online) (a) External (black) and internal (red) boundaries of the plate on the underside. The internal boundary corresponds to the beginning of the internal arched region. (b) Section of the parametric generated bass bar, where a changing in its height can be observed.

the plate, where the inside arching begins, indicated by the red line in Fig. 4(a). To determine it, we first remove the four corners of the edge. The identification of the corner positions is done in an automatic fashion, through the computation of the convex hull area for short segments of the boundary. The evaluation of this function presents four peaks along the edge, which correspond to the location of the four corners, as shown in Fig. 5. We remove all the points in a radius of 25 mm from the corners and then interpolate the result to fill the gaps. The interpolation is accomplished through a spline of order 4. The result is a guitar-shaped boundary. Finally, all the points along the boundary are translated along the normals of the edge toward the centre of the violin by a distance of 7 mm, thus creating a region at the edges of the inner surface of the top. This region is

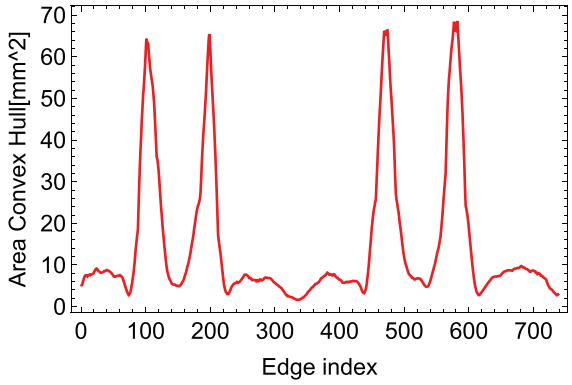

FIG. 5. (Color online) Area of the convex hull mesh for all the points in a radius of 10 mm along the edge. Data are smoothed with a moving average of 15 points, and total number of points on the edge is 720 (a sampling frequency of 0.7 point/mm).

flat and corresponds to the area where the ribs are glued to the plate.

Depending on the violin maker, the lower (tailpiece) and the upper (neck) regions either follow the shape of the end blocks or are left straight. We decided for the latter option, as shown by the red line in Fig. 4(a). The reader is encouraged to see Fig. 1 of Stoel and Borman (2008) for a more complete overview on the strategies followed by makers. All the numerical values used here are taken according to Blahout (2020), since we do not have access to the interior of the Messiah.

The points of the inner surface of the plate are found starting from the points of the outer one. They are divided into two groups, depending on whether they are inside or outside the inner boundary on the xy plane. This is done to separate the flat region from the arched one in the inner surface.

The z coordinates of the points in the inner surface are found in different ways for the two regions. In the flat one, all the points of the inner surface lying between the black and the red lines in Fig. 4(a) share the same z coordinate, thus making a variable thickness edge. In the region internal to the red line, we have to compute the z coordinate of each point starting from the points of the outer surface. In this process, the considered points are the ones that are inside the red line in Fig. 4(a). Starting from this boundary, a margin of 5 mm is added, to have some space between the two regions that guarantees a smooth transition between them. Then all the points of the upper surface are translated downward in the z direction by a constant value of 2.7 mm, thus making a top with constant thickness.

The two different regions are then joined together to obtain the complete inner surface. This is done through a linear interpolation that fills the gaps that are present. During this procedure, the arching boundary is taken as a constraint, so that the flat area of the surface is preserved. The interpolation method used is of differentiability class C^0, so we are sure that any discontinuity is avoided on the surface.

Finally, the distribution of the points in the arched region of the inner surface is homogenised with the same diffusion-like method used for the edge of which a 1D example is shown in Fig. 6 for a varying number of smoothing iterations. Using this algorithm is a rather convenient choice, since it keeps the large-scale characteristics of the system and is not qualitatively dependent on the number of iterations. This lets us obtain smooth transitions between all the areas of the inner surface and nice regular contour lines, just like actual violins.

Inner and outer surfaces are assembled into a single volume by computing its alpha shape (Edelsbrunner *et al.*, 1983), from which the final mesh is obtained. The f-holes are obtained by a simple mesh subtraction, between the plate and an extruded version of the hole's geometry. The shape of the f-hole is obtained by projecting the violin top into the xy plane and tracing its boundary. The addition of the bass

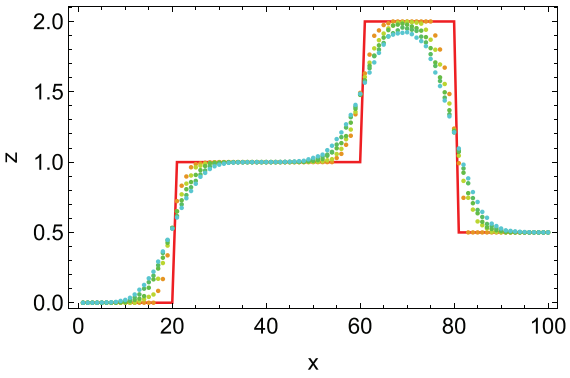

FIG. 6. (Color online) Smoothing algorithm in action in a 1D discontinuous function (red line). For each set of points, we have applied 500 iterations, between 0 and 2500.

bar is slightly more complicated and will be explained in detail in what follows.

C. Varying thickness

The thickness of the violin plates is perhaps one of the most researched features by violin makers and probably one of the least understood. It is a fact that the eigenfrequencies of the modes of the plates depend on the local thickness distribution of the plate. This can be seen in studies that track the modal shapes in different building stages (Schleske, 1996) or the relation between thickness and sound (Buen, 2006). Furthermore, there is historical evidence that makers used different thickness patterns in their works (Stoel and Borman, 2008), different rules for the mode frequency ratios (Harris, 2005), or different plate stiffness (Hutchins, 1981).

In our approach, the area inside the arching boundary is divided into nine sub-regions that can be controlled independently with different thicknesses. This division is used to approximate the actual historical examples (Stoel and Borman, 2008). Three regions each are located in the upper and the lower bouts; one corresponds to the waist and two to the f-holes. In this way, when the plate is built, we can decide the thickness of nine different areas.

The generation of the inner surface is performed in the same way as in the case of constant thickness, with the only difference being that when the points in the arched region are translated downward, the z-value of the translation varies for each point, depending on the region to which it belongs.

Finally, a homogenisation process, an example of which is shown in Fig. 6, is performed on the sections both along the x and y directions, so that the resulting surface does not present discontinuities between regions with different thicknesses. Notice how this approach makes the top plate much more realistic if compared with previous studies (Tinnsten and Carlsson, 2002; Razeto *et al.*, 2006; Torres *et al.*, 2020).

D. Bass bar

The bass bar is a brace running almost parallel to the y direction, glued to the inner surface and passing below the bass foot of the bridge. It bears much of the tension of the strings. The location, shape, and wood orientation of the bass bar vary greatly in historical examples. In the baroque era, the bass bar was shorter, thinner, and lower than today's standard, in part due to the use of gut strings, whose tension was far less than contemporary metal wound strings. In contemporary violin making, the bass bar dimensions are more or less standardised in a length of 270 mm, 5.5–6 mm width, and 13 mm height at its highest point. The location is determined geometrically and is slanted around 3° next to the upper hole of the left f-hole. The position of the bass bar is something luthiers usually modify in search of a certain tone. We study here the effect of slanting on the normal modes. The mesh of the bass bar is generated in a parametric manner, so that we can control width, length, positioning, rotation with relation to the plate and heights at seven different points. For the transverse cross section, we use a quartic polynomial to mimic the real bass bars.

The side of the bar attached to the plate is synthesised starting from the (x, y, z) coordinates of the inner surface of the top plate. This decision is taken so that plate and bar will adhere perfectly to each other, speeding up the simulation procedure. In addition to this, to improve the results, the resolution of the mesh is increased along the area in contact with the bottom of the bass bar. Figure 7 shows three different parametric bass bars, where the length, width, and height have been varied.

III. PREDICTION OF THE VIBRATIONAL BEHAVIOR

In this section, we use the synthetic mesh created according to the procedure described in Sec. II to predict the vibrational behavior of the plate (Fig. 8).

The material used for the simulations is Sitka Spruce, not a common material in European violin making tradition, but with mechanical properties similar to tonewood (Ross, 2010). The same wood is used also for the bass bar, but, since is it not aligned to the plate, we have to pay attention to its grain orientation, rotating it to the same angle of rotation as the bar.

Since the wood is an orthotropic material, we have to define different properties for the different directions. The considered values are taken according to Ross (2010) and can be seen in Table I, while the considered density is equal to 450 kg/m^3.

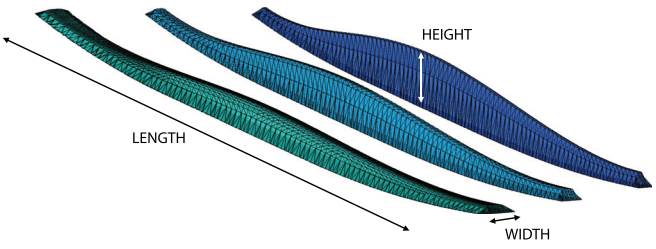

FIG. 7. (Color online) Meshes of three different parametric bass bars, where the parameter values are varied accordingly to the colour gradient of the meshes. From green to blue, the length and the width of the bar are reduced, while the height is increased.

https://doi.org/10.1121/10.0003599

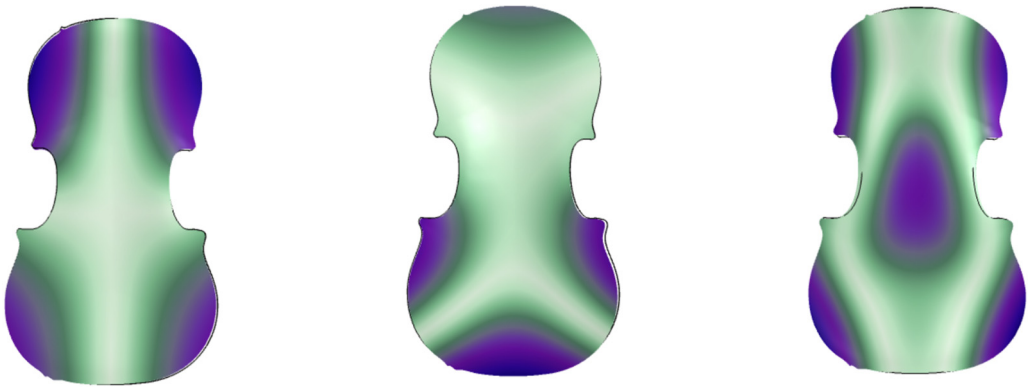

FIG. 8. (Color online) From left to right: modal shapes for modes 1, 2, and 5 for the case without bass bar and constant thickness $h = 2.7$ mm.

The mechanical behavior is studied through a FEM simulation performed with COMSOL MULTIPHYSICS® software, performing an eigenfrequency study in solid mechanics physics. Each generated mesh is imported and analysed in free boundary conditions with a tetrahedron mesh automatically generated by the software.

The results presented here have been obtained with one set of material parameters. We have also realised the same simulations with different material properties (i.e., different wood), and the results are quantitatively different but qualitatively similar. In particular, our optimisation for the thickness of the top shows a similar thickness pattern for the other material studied. We think that repeating the results with a set of material properties is not so interesting in the general case but sheds light on the fact that for each particular piece of wood, the "optimal" inner surface will be slightly different for any given geometry.

IV. RESULTS

A. Ratio f_5/f_2 with and without f-holes

The role of the f_5/f_2 ratio has been discussed in Curtin (2005), for top plates with the f-holes cut and the bass bar either installed or not. Since luthiers usually cut the f-holes after graduating the top plate, we decided to study the variation of the frequency ratio with and without f-holes. Furthermore, it is computationally easier to simulate without the f-holes, so we will base our optimisation in the estimated value for the ratio. Figure 9 shows the relation between the ratio for top plates with and without f-holes. We have randomly varied the thickness, according to eight independent Gaussian distributions, with a mean of 2.7 mm and a variance of $\sigma = 0.25$ mm. The results show that the ratios are rather linearly related, and the f-holes lower the value of the ratio by approximately 25%.

TABLE I. Values of the orthotropic properties of the simulated material, density 450 kg/m^3.

Young's modulus (GPa)	Rigidity modulus	Poisson's ratio
$E_y = 10.8$	$G_{yx}/E_y = 0.061$	$\mu_{yx} = 0.467$
$E_x/E_y = 0.043$	$G_{xz}/E_y = 0.064$	$\mu_{xz} = 0.372$
$E_z/E_y = 0.078$	$G_{yz}/E_y = 0.003$	$\mu_{yz} = 0.435$

B. Varying thickness

To approach the problem of the optimisation of the thickness profile in a gradual fashion, we start by varying the thickness in the upper and lower bouts (T_u and T_b, respectively) and waist as a whole, thus creating only three different thickness regions: upper, middle, and lower. Of these three regions, we study the variation of the eigenfrequencies only for the upper and lower bout thicknesses, denoted by T_u and T_b, respectively. We analyse the impact of the thickness on the eigenfrequencies of the signature modes, namely modes 1, 2, and 5, denoted by f_1, f_2, and f_5, respectively.

The results can be summarised as follows:

- Mode 1: the eigenfrequency f_1 grows almost linearly with $T_u + T_l$ from 58 Hz for a thickness of 2 mm to 68 Hz for a thickness of 3 mm.
- Mode 2: the eigenfrequency f_2 depends mostly on T_l and varies from 100 to 115 Hz.
- Mode 5: the eigenfrequency f_5 shows the greatest variation, linear with $T_u + T_l$ from 240 to 275 Hz.

In Fig. 10, we plot the ratio f_5/f_2, as obtained from the simulations for T_u and T_b varying independently in the interval 2.0–3.0 mm. We can observe a nonlinear dependence with iso-curves for values in the range of the historical examples. Since the dependence of the ratio is nonlinear, it is not possible to study the behavior of the modes only by moving one variable at a time, as it has currently been done in the literature (Gough, 2015; Razeto *et al.*, 2006). Because of this, we decided to study the dependence of the frequency ratio f_5/f_2 as a minimisation problem, which is the subject of Sec. IV C.

C. Optimising thickness

Violin makers work with a precision of tenths of a millimetre, so an exhaustive variation of the thickness of the nine regions we have defined is computationally intractable. A better way to proceed is to run a minimisation procedure

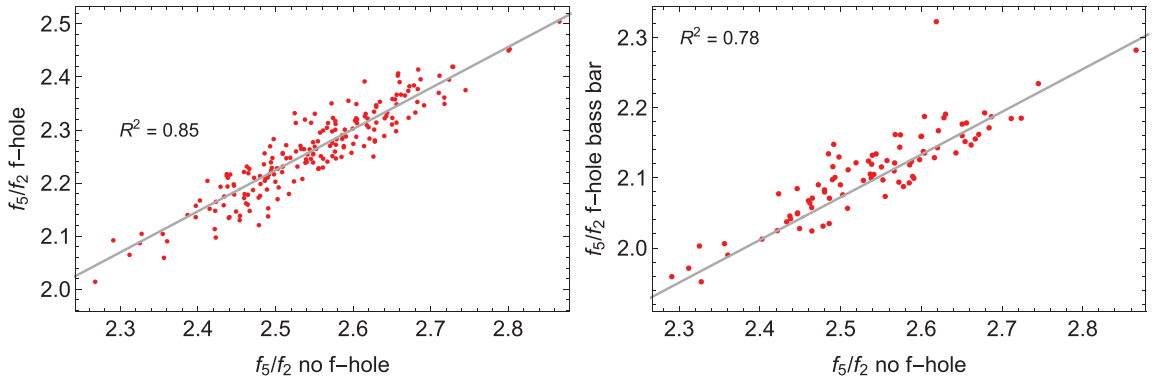

FIG. 9. (Color online) Ratio f_5/f_2 for 250 top plates with different thicknesses profiles (distributed normally around constant 2.7 mm thickness) for the case with and without f-holes. The f-holes are always located in the same position. We have dropped two outliers for the plot with bass bar and f-holes.

where the violin top is simulated only at the steps of the multidimensional path created by the minimisation, rather than a grid in the nine-dimensional space. We have used MATLAB as a scripting language for the COMSOL simulations, so in each step of the optimisation we create a mesh in MATLAB, compute its eigenvalues in COMSOL, and evaluate the loss function and the gradients again in MATLAB. Figure 11 shows the algorithm and where each stage of the computation is performed. To further simplify the computation, we developed our own pseudorandom gradient method. For the first iteration, we compute the gradient in all of the nine directions. For the following iterations, we move in the direction of the steepest descent (at a fixed $\mu = 0.02$ mm) in the three most varying directions of the previous step plus two random ones.

To obtain a more extensive insight into the vibrational behavior of plates, we did not limit the optimisation to the f_5/f_2 ratio, but we applied this method to three different loss functions, namely,

$$L_1 = |2.5 - f_5/f_2|^2, \tag{2}$$

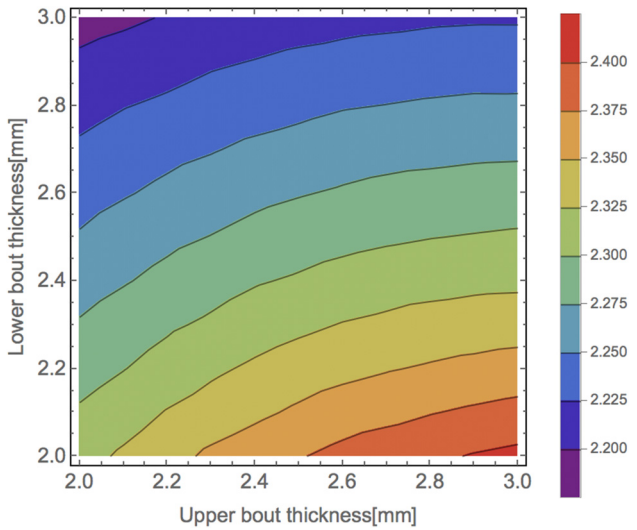

FIG. 10. (Color online) Ratio f_5/f_2 as a function of the thickness in the upper T_u and lower bout T_b.

which is the loss function associated with an octave relation between the complete top plate's second and fifth frequency. The 2.5 value is chosen as a ballpark figure that will give a ratio close to 2 when the bass bar and f-holes are added. Second, we define

$$L_2 = \frac{1}{N-1}\sum_{i=2}^{N}\left(\frac{f_i}{f_{i-1}} - \mu\right)^2, \tag{3}$$

with $N = 10$ and $\mu = (1/N-1)\sum_{i=2}^{N} f_i/f_{i-1}$ the average of the frequency ratios. And finally,

$$L_3 = \frac{m}{\hat{m}}|f_5 - \hat{f}_5|, \tag{4}$$

where $\hat{f}_5$ is the average fifth frequency, m is the mass of the plate, and $\hat{m}$ the average mass. The quantities $\hat{f}$ and $\hat{m}$ have been obtained as the average values for a dataset of 250 top plates, where the thickness distribution is varied according to a Gaussian distribution of zero mean and variance of 10%, each region independently of each other.

The role of L_1 has been discussed in Curtin (2005), and it corresponds to a simple modal relation that can be computed by the violin maker in the construction process. The loss function L_2 corresponds to a top that has its eigenfrequencies "tuned" as closely as possible as an equal tempered instrument. Notice that we are not requiring the frequencies to be at a specific value or that they be at semitone distance, but only that they be equally spaced in the (logarithmic) frequency domain. We use this function as an example of a loss function that takes into account several eigenfrequencies, and not just the values of one or two, as seems to be the norm in the literature. The loss function L_3 derives from the observation that minimising the impedance is equivalent to reducing the mass of the top while keeping the frequency of the fifth mode close to the average value for the given material. In other words, it is akin to selecting a top with lower density, which is preferred by violin makers. This loss function is interesting because it relies not only on the eigenfrequencies to be computed, but also on the mass of the top plate, and shows how our method could be used to maximise functions that belong to other domains beyond the

https://doi.org/10.1121/10.0003599

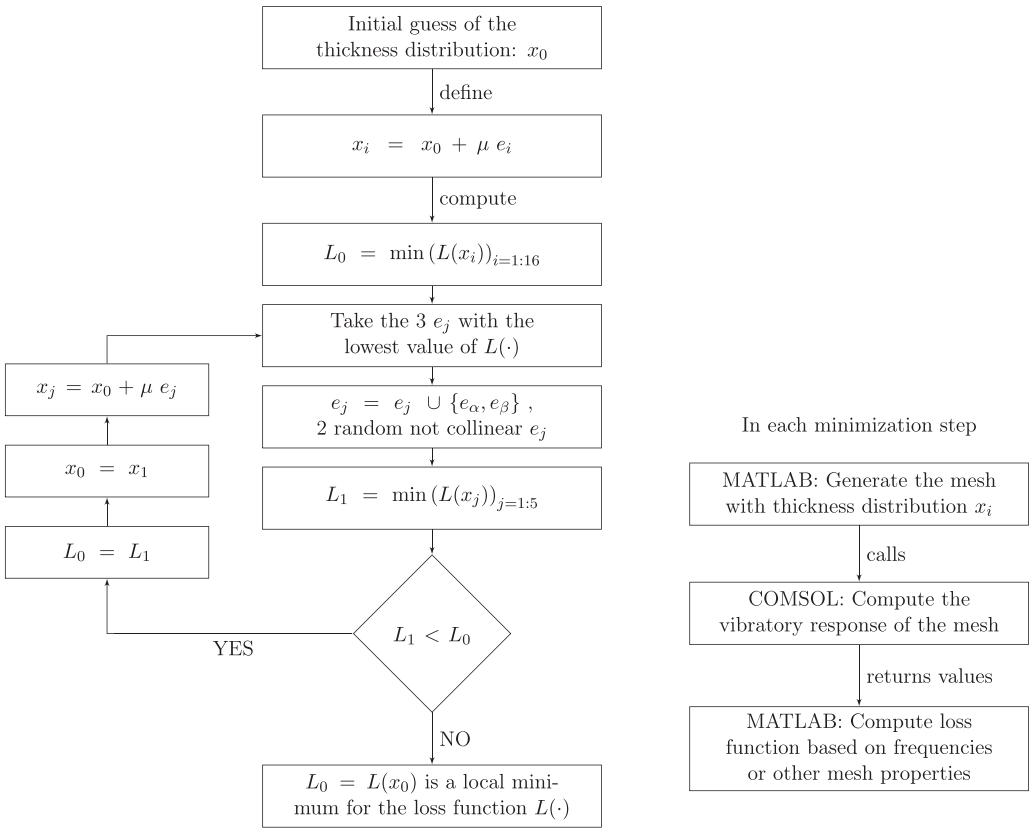

FIG. 11. Left: flow chart of the modified steepest descent method used. Right: computation of the loss function $L(\cdot)$ and interaction between MATLAB and COMSOL.

vibrational. This is important because what luthiers search to optimise is the tone and sound of a violin, not its vibrational frequencies—the latter only valuable as a proxy of the former.

Figure 12 shows the thickness map for the final stages of each minimisation using a colour scale. Notice how the optimal solution for L_1, shown in Fig. 12(a), is to increase the thickness at the waist in the central region, with smaller variations in the upper and lower bouts. On the other hand, in Fig. 12(b), for the optimisation of L_2, we have that the thickness must increase in the central region of the lower bout and decrease at the left and right regions of the upper bout. Finally, Fig. 12(c) shows that to minimise L_3, we have to make thinner the central region of the waist and the two lateral regions of the lower bout. In all of the three cases, the thickness distribution of the plate is symmetric with respect to the vertical axis. This is not always the case when the bass bar is added, as we will see below.

D. Bass bar length and angle

We now analyse the vibrational behavior with respect to the bass bar length and positioning. For simplicity, we focus on the dependence of the frequency on the first few

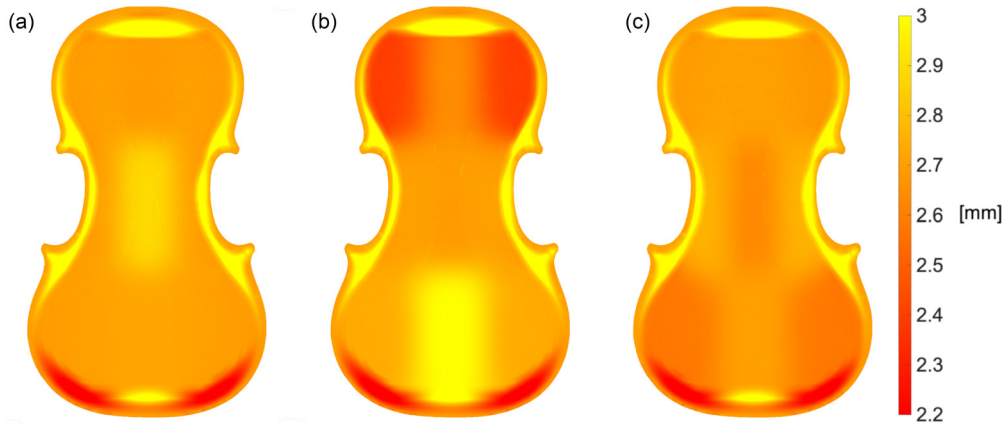

FIG. 12. (Color online) Thickness map for the minimisation procedures we have realised: (a) shows the result for L_1, (b) for L_2, and (c) for L_3, all starting from homogeneous thickness.

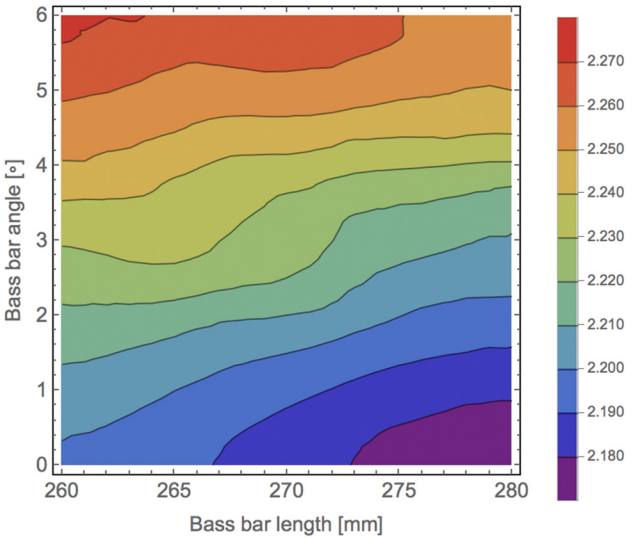

FIG. 13. (Color online) Ratio f_5/f_2 as a function of α and L. Notice how the ratio is not a bijective function of the length for some angles, in particular how for $\alpha = 3^\circ$ there is an interval of lengths that generates the same f_5/f_2 ratio.

modes of the top plate as a function of the angle α and length L_b of the bass bar. The first mode is mostly independent of L_b and increases with increasing α from 134 to 140 Hz. Higher modes have a bi-linear behavior, and interestingly, the dependences of f_2 and f_5 on α are inverted, giving rise to a region of parameters that comply with the ratio found in old Cremonese violins (Curtin, 2005).

More specifically, Fig. 13 shows the ratio f_5/f_2 for varying α and L_b. The ratio increases when decreasing L_b and when increasing α; therefore, one could modify the length of the bass bar to compensate for a different orientation of it. In this way, one has two parameters to modify independently the first mode f_1 and the ratio f_5/f_2. The results are consistent with the values found in historical Cremonese violins (Curtin, 2005) and, to the best of our knowledge, not reported before.

E. Positioning and size

Finally, we investigate the influence of the displacement from their nominal position and variations in the other size dimensions of the bass bar. The reference values for the geometry of the bar are 13 mm for the central height, length of 276 mm, and width of 6 mm. With regard to the positioning, the centre of the bar is shifted with respect to that of the plate by 5 and 16 mm in the vertical and horizontal direction, respectively. The coordinates of the plate and bar correspond to those of their centres of mass. The bar is rotated with respect to the vertical axis by 3° counterclockwise. The values of all variables are taken according to Blahout (2020). When we vary the width of the bass bar by 15%, the ratio f_5/f_2 is only affected by 0.5%. Likewise, for the height of the bass bar, that was varied between 9 and 19 mm. The height does affect the absolute value of the frequencies more than other variables, but not the ratio f_5/f_2. The width of the bar only significantly changes the frequency of the first mode. This shows that not all the variables in the design are equally important, and one does not need to study them extensively. On the other hand, the variation of the position of the bass bar on the plate does not affect the eigenfrequencies significantly. Figure 14 shows that by moving the centre of the bar by half of its width in both vertical and horizontal directions, the frequencies vary by less than 2%.

F. Optimising the thickness profile with the bass bar

Figure 15 shows the optimal thickness profile for the three loss functions when the presence of the bass bar is considered. The thickness distributions are no longer symmetric in the first two cases. The minimisation of L_1 leads to an asymmetry that is concentrated mostly in the lower bout, whereas the minimisation of L_2 leads to asymmetric lower and upper bouts. Conversely, when minimising L_3, we obtain a symmetric thickness profile with respect to the vertical axis, showing that not all the optimal thickness distribution needs to be asymmetric to compensate for the asymmetry induced by the presence of the bass bar.

V. CONCLUSIONS

We have studied the vibrational behavior of free violin plates for a wide range of design parameters and identified

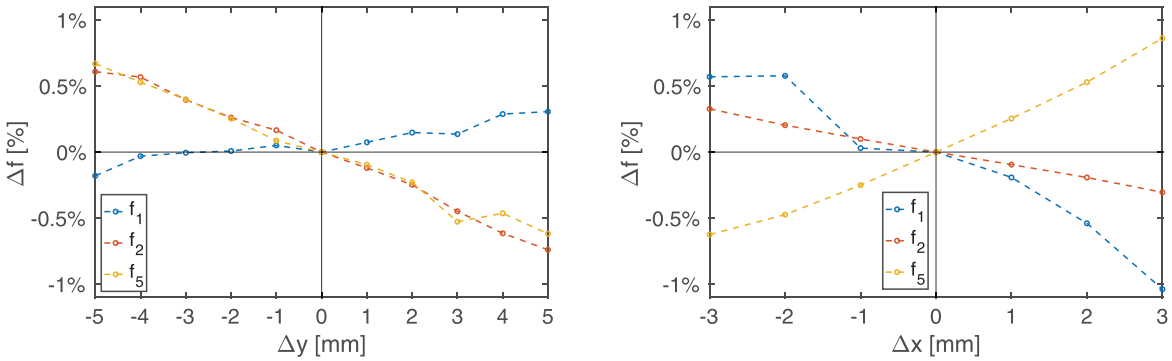

FIG. 14. (Color online) Percentage variation of the eigenfrequency values of the first, second, and fifth modes for varying positions of the bass bar. The values on the x axis indicate the vertical (left) and horizontal (right) displacement of the centre of mass of the bar from its standard position. All the values are normalised with respect to those of the standard position of the bar.

https://doi.org/10.1121/10.0003599

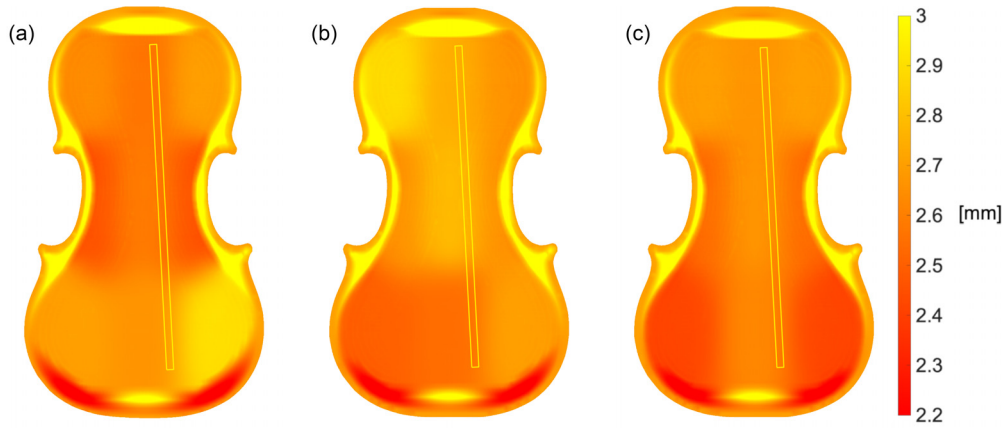

FIG. 15. (Color online) Thickness map for the minimisation procedures we have realised, considering the presence of the bass bar: (a) shows the result for L_1, (b) for L_2, and (c) for L_3, all starting from homogeneous thickness.

those with the greatest influence in the frequencies of the eigenmodes.

The violin tops have been created from a 3D scan of a historical violin, and the methodology to achieve this has been presented. This procedure is not trivial and to the best of our knowledge has not been presented before. The resulting meshes are far more accurate than the state of the art, and, in particular, special care was taken to correctly reproduce the bass bar and ensure that the modifications to the height in the inside arching are coherent with the actual practice of luthiers [in contrast to previous studies (Gough, 2015; Tinnsten and Carlsson, 2002)]. We have studied the dependence of the ratio f_5/f_2 on several parameters and showed it to give values close to actual historical ones. This methodology can be used by luthiers in the building process to determine the optimal inner shape of any given model.

We have explained why the heuristic of violin makers works when aiming for a $f_5/f_2 = 2.5$ for the unfinished plate and what is the quantitative effect of f-holes and bass bar on the modes of the plate. Furthermore, our results show that the effect of different variables in f_5/f_2 is not just a linear combination of each. This should be expected for a complex system like the violin. One caveat of our results is that they are valid for the particular "model" of violin that we have studied. Different makers use different shapes for the outline and outer arching. We expect that the way the modes depend on the different parameters will also vary when varying the model of the violin. To prove this, we have run the optimisation procedure for a slightly different outer arching, and the results are both quantitatively and qualitatively different (data not shown).

Finally, we have shown that it is possible to optimise the top plate thickness to minimise arbitrary loss functions. In general, when the bass bar is not considered, the optimal thickness profile is symmetric with respect to the vertical axis. When the bass bar is included, the optimal thickness profile is not necessarily symmetric.

Our methodology opens the door to a multidimensional optimisation of the violin response by means of simulation. We have studied the modal response of the free top plate, but the methodology works with any loss function. In particular, the full body modes or the radiance pattern (Canclini *et al.*, 2020) come to mind. Different loss functions can be defined with the help of professional luthiers and informed by the characteristics present in historical violins. Then one can find the violin shape that optimises this loss function. In this way, by simulating the interplay of all the design (and perhaps material) parameters of a violin, we will be closer to understanding the mystery behind what makes some wood, glue, and varnish sound the way they do when worked by the skilful hands of a master.

ACKNOWLEDGMENT

We thank the Museo del Violino foundation in Cremona for giving access to the Messiah when it was exposed there. We also want to thank Gregg Alf for coordinating the organisation of the measurement session and the Ashmolean Museum for authorising the scanning of the instrument. We thank the "Arvedi Non-Invasive Diagnostic Lab" at the University of Pavia for sharing the data and violin maker Manuel Di Landa for fruitful discussions regarding the effect of the bass bar on the violin tone. The work in this publication has been partially funded by the Violin Making Cultural District of Cremona.

Blahout, V. (**2020**). "The violin making manual," http://www.makingthe-violin.com/ (Last viewed 3/2/2021).

Bretos, J., Santamaria, C., and Moral, J. A. (**1999**). "Vibrational patterns and frequency responses of the free plates and box of a violin obtained by finite element analysis," J. Acoust. Soc. Am. **105**(3), 1942–1950.

Buen, A. (**2006**). "Can we hear the geometrical measures of a violin?," in *Proceedings of the Joint Baltic-Nordic Acoustics Meeting (BNAM)*, Gothenburg, Sweden, pp. 1–15.

Buksnowitz, C., Teischinger, A., Müller, U., Pahler, A., and Evans, R. (**2007**). "Resonance wood [*Picea abies* (L.) Karst.]—Evaluation and prediction of violin makers' quality-grading," J. Acoust. Soc. Am. **121**(4), 2384–2395.

Cacciatori, F. (**2016**). *Antonio Stradivari. Disegni, Modelli, Forme. Catalogo Dei Reperti Delle Collezioni Civiche Liutarie Del Comune di Cremona. Con DVD. Ediz. italiana e Inglese* (MdV-Museo del Violino, Cremona, Italy).

Canclini, A., Antonacci, F., Tubaro, S., and Sarti, A. (**2020**). "A methodology for the robust estimation of the radiation pattern of acoustic sources," IEEE/ACM Trans. Audio Speech Lang. Process. **28**, 211–224.
Chatziioannou, V. (**2019**). "Reconstruction of an early viola da gamba informed by physical modeling," J. Acoust. Soc. Am. **145**(6), 3435–3442.
Curtin, J. (**2005**). "Tap tones and weights of old Italian violin tops," J. Violin Soc. Am. **20**(2), 161–174.
Davis, E. B. (**2013**). "On the effective material properties of violin plates," in *Proceedings of the Stockholm Music Acoustics Conference 2013*, July 30 to August 3, Stockholm, Sweden.
Edelsbrunner, H., Kirkpatrick, D., and Seidel, R. (**1983**). "On the shape of a set of points in the plane," IEEE Trans. Inf. Theory **29**(4), 551–559.
Fritz, C., Curtin, J., Poitevineau, J., Borsarello, H., Wollman, I., Tao, F.-C., and Ghasarossian, T. (**2014**). "Soloist evaluations of six Old Italian and six new violins," Proc. Natl. Acad. Sci. U.S.A. **111**(20), 7224–7229.
Fritz, C., Curtin, J., Poitevineau, J., Morrel-Samuels, P., and Tao, F.-C. (**2012**). "Player preferences among new and old violins," Proc. Natl. Acad. Sci. U.S.A. **109**(3), 760–763.
Fritz, C., Woodhouse, J., Cheng, F. P.-H., Cross, I., Blackwell, A. F., and Moore, B. C. (**2010**). "Perceptual studies of violin body damping and vibrato," J. Acoust. Soc. Am. **127**(1), 513–524.
Gore, T., and Gilet, G. (**2016**). *Contemporary Acoustic Guitar Design and Build*, 2nd ed., Vol. 1 (Trevor Gore, Terrey Hills, Australia).
Gough, C. (**2015**). "Violin plate modes," J. Acoust. Soc. Am. **137**(1), 139–153.
Harris, N. (**2005**). "On graduating the thickness of violin plates to achieve tonal repeatability," VSA Papers **1**(1), 111–120.
Hutchins, C. M. (**1981**). "The acoustics of violin plates," Sci. Am. **245**(4), 170–187.
Knott, G., Shin, Y., and Chargin, M. (**1989**). "A modal analysis of the violin," Finite Elem. Anal. Des. **5**(3), 269–279.
Molin, N.-E., Lindgren, L.-E., and Jansson, E. V. (**1988**). "Parameters of violin plates and their influence on the plate modes," J. Acoust. Soc. Am. **83**(1), 281–291.
Nia, H. T., Jain, A. D., Liu, Y., Alam, M.-R., Barnas, R., and Makris, N. C. (**2015**). "The evolution of air resonance power efficiency in the violin and its ancestors," Proc. Math. Phys. Eng. Sci. **471**(2175), 20140905.
Razeto, M., Staforelli, C., and Barrientos, G. (**2006**). "Sensibility analysis of violin plates," in *Computational Methods in Engineering and Science* (Springer, Berlin), pp. 333–333.
Ross, R. J. (**2010**). *Wood Handbook: Wood as an Engineering Material*, General Technical Report GTR-190 (United States Department of Agriculture, Forest Service, Forest Products Laboratory, Madison, WI).
Sacconi, S., Dipper, A., and Rivaroli, C. (**1979**). *The Secrets of Stradivari* (Libreria del Convegno, Milan, Italy).
Schelleng, J. C. (**1968**). "Acoustical effects of violin varnish," J. Acoust. Soc. Am. **44**(5), 1175–1183.
Schleske, M. (**1996**). "Eigenmodes of vibration in the working process of a violin," Catgut Acoust. Soc. J. **3**(1), 2–8.
Setragno, F., Zanoni, M., Antonacci, F., Sarti, A., Malagodi, M., Rovetta, T., and Invernizzi, C. (**2017**). "Feature-based analysis of the impact of ground coat and varnish on violin tone qualities," Acta Acust. United Acust. **103**(1), 80–93.
Staforelli, C., Razeto, M., and Pascual, R. (**2002**). "Numerical and experimental analysis on the dynamic behaviour of the violin plates," in *Proceedings of the 2002 International Conference on Noise and Vibration Engineering*, ISMA, September 16–18, Leuven, Belgium.
Stoel, B. C., and Borman, T. M. (**2008**). "A comparison of wood density between classical Cremonese and modern violins," PLoS One **3**(7), e2554.
Tai, H.-C., Shen, Y.-P., Lin, J.-H., and Chung, D.-T. (**2018**). "Acoustic evolution of old Italian violins from Amati to Stradivari," Proc. Natl. Acad. Sci. U.S.A. **115**(23), 5926–5931.
Tinnsten, M., and Carlsson, P. (**2002**). "Numerical optimization of violin top plates," Acta Acust. United Acust. **88**(2), 278–285.
Torres, J. A., Soto, C. A., and Torres-Torres, D. (**2020**). "Exploring design variations of the Titian Stradivari violin using a finite element model," J. Acoust. Soc. Am. **148**(3), 1496–1506.
Woodhouse, J. (**2014**). "The acoustics of the violin: A review," Rep. Prog. Phys. **77**(11), 115901.
Yu, Y., Jang, I. G., Kim, I. K., and Kwak, B. M. (**2010**). "Nodal line optimization and its application to violin top plate design," J. Sound Vib. **329**(22), 4785–4796.